




Editorial

# Advances in Remote Sensing-Based Disaster Monitoring and Assessment

Jungho Im <sup>1,\*</sup>, Haemi Park <sup>1,2</sup> and Wataru Takeuchi <sup>2</sup>

<sup>1</sup> Ulsan National Institute of Science and Technology, Ulsan 44919, Korea

<sup>2</sup> Institute of Industrial Science, The University of Tokyo, Tokyo 153-8505, Japan; hmpark@iis.u-tokyo.ac.jp (H.P.); wataru@iis.u-tokyo.ac.jp (W.T.)

\* Correspondence: ersgis@unist.ac.kr

Received: 10 September 2019; Accepted: 16 September 2019; Published: 19 September 2019



Extreme weather/climate events have been increasing partly due to on-going climate change. Such events become disasters where people live. In a sustainable society, the rapid detection and monitoring of natural disasters are required. Remote sensing techniques are suitable for dealing with natural disasters that have various characteristics in multiple spatial and temporal domains. Continued efforts in finding ways to operationally-monitor and assess disastrous events such as heavy rains, floods, drought, heatwave, and forest fires are consistently rewarded by integrating advanced remote sensing. However, the development of robust disaster monitoring and assessment methods from regional to national scales of disasters is still challenging as disastrous events typically result from complex mechanisms. A multitude of data from visible to microwave remote sensing have been used for conducting comprehensive monitoring and assessment solutions for disasters. Disaster monitoring and assessment are the areas that have benefited most by recent advances in satellite, airborne, and ground remote sensing. Novel techniques in image analysis and the scheduled launch of a series of new sensors with enhanced specifications are also promising for disaster monitoring and assessment, which aims at reducing the risks caused by disasters. This special issue aims at finding novel approaches using various satellite-based images and airborne/ground instruments for the monitoring and assessment of natural disasters including floods, droughts, cyclones, landslides, and land subsidence.

## 1. Overview of Contributions

Myoung et al. [1] modeled live fuel moisture (LFM) using the enhanced vegetation index (EVI) of the moderate resolution imaging spectroradiometer (MODIS). The LFM is a conventional index for indicating the danger level of wildfires. Linear models between EVI and other meteorological factors and in situ LFM observations in California were developed in the study. There was a stronger relationship between LFM and EVI when ancillary meteorological predictors were considered together when compared to the model that only used the EVI. It was confirmed that the temporal discrepancy between in situ measurements and satellite data has substantial impact on the accuracy of LFM estimation. Furthermore, the spatial consistency between the in situ and satellite-based datasets were examined. The proposed method was tested with the Coby fire that occurred in January 2014 in California, USA. The fire ignition point and the burnt area were well matched with the place where the LFM showed under 60%, which was considered as highly dangerous for wildfires.

Ryu et al. [2] investigated the usefulness of satellite-based burned ratios and vegetation indices to explore post-fire recovery processes. Normalized burned ratio (NBR) and the difference between pre- and post-fire NBRs were calculated using a MODIS product (i.e., MOD09 collection 6) of Terra. The burned ratio of wildfire not only affects the loss of carbon resource, but also the carbon assimilation ratio. For that, the gross primary production (GPP) of MODIS (MOD17A2H) was additionally compared to monitor the post-fire recovery processes. These metrics were able to visualize the phenomena of forest recovery in South Korea, which experienced a severe fire event in 2004.

Yang et al. [3] investigated the relationship between urban structures and land subsidence using the Envisat advanced synthetic aperture radar (ASAR) and TerraSAR-X high resolution SAR data. In Beijing, an intensively developed urban area, the high-rise building areas showed significant land subsidence when compared to the areas of low-rise buildings. The permanent scatter interferometric synthetic aperture radar (PS-InSAR) technique was harmonized with high resolution SAR data and in situ observations to reveal the mechanisms of land subsidence under the urban areas. The novelty of this study lies in the block scale analysis with the advantage of using high resolution SAR.

Lim and Lee [4] simulated flood damage areas (FDAs) in North Korea by taking advantage of satellite-based information derived from inaccessible areas. Expert-based multiple remote sensing and GIS approaches were chosen for the delineation of flood inundated areas (FIAs) referenced to visible Google Earth high resolution imagery. Sentinel-1 radar images were used to detect the FIAs. The stream flows along the geomorphology were modeled by the Geomorphon model. The originality of this study was included in the model selection by using multiple combinations of input variables. Finally, the most robust model was able to delineate FDAs, which agreed well with the damage information in the reports provided by the North Korean government.

Ma et al. [5] established a flash flood risk model in Yunnan Province in China, a typical flood-prone area. Unlike typical floods, flash floods are known to be highly risky, making it difficult for people to evacuate their residences. The model was developed using satellite-based meteorological, topographical, hydrological, and anthropological indices as the input factors affecting flash floods by using an artificial intelligence algorithm, named the least squares support vector machine (LSSVM). The highest model performance in terms of accuracy was achieved by the LSSVM with a radial basis function (RBF) kernel. In particular, the curve number in the topographical factors was the most contributing factor to the flash flood risk model. The choice of model input variable and model verification were carefully conducted and high risk areas were identified through the risk analysis.

Jang et al. [6] developed a forest fire detection model using geostationary satellite images, Himawari-8 AHI, over South Korea. The model consisted of thresholding, random forest machine learning, and post-processing. In South Korea, wildfires frequently occur at a small scale. For this reason, accurate and rapid forest fire detection using high spatial and temporal resolution satellite data is crucial. However, existing approaches have several critical limitations including a very high false alarm rate. The three-step fire detection model proposed in this study focused on maintaining a high probability of detection (>90%) without increasing a false alarm rate (i.e., significant reduction of a false alarm rate when compared to the existing approaches). The proposed model was validated with real fire events, resulting in a good performance even for small scale fires.

Zhang et al. [7] proposed a new dryness monitoring indicator, the ratio dryness monitoring index (RDMI). Surface dryness monitoring is important to assess water deficiency as a disaster to harm human lives and ecosystems. The RDMI was developed using distances from the “Edges on the triangle” on the near-infrared (NIR) and Red reflectance feature space since the NIR and Red wavelengths are closely related to moisture and vegetation. In particular, defining wet and dry edges using NIR and Red reflectance is a novel component when compared to existing surface dryness indices. The proposed approach was demonstrated in Xinjiang, China, where the biggest desert in Asia is located. The results showed a conspicuous agreement with the distribution of landcover types.

Zuo et al. [8] combined two SAR data, Envisat ASAR and Radarsat-2, with the PS-In SAR method to capture the temporal patterns of land subsidence and demonstrated the stage of land subsidence in terms of temporal evolution in the east of the Beijing Plain in China, which is known as an area that has largely subsided. A permutation entropy method was used to reverse the temporal evolution pattern of land subsidence. The rate of subsidence results from the SAR timeseries was validated with in situ data resulting in high accuracy ( $R^2 = 0.94$ ). The time-series of land subsidence showed uneven patterns and agreed well with the decreasing pattern of groundwater, although the subsidence would progress along with the geological conditions. Finally, the overexploitation of groundwater was considered as the main cause of land subsidence from this temporal analysis.

Tropical cyclones (TCs) are one of the most risky disasters in terms of casualties and economic losses. However, the determination of TC initiation still requires human interpretation. Several studies have been conducted to automate the process of identifying whether a TC will develop. Kim et al. [9] developed an automatic TC initiation detection model with machine learning (ML) approaches and compared those methods using four metrics: heat rate, false alarm rate, Peirce skill score, and lead time. The ocean surface wind and precipitation from WindSat were used to build three ML-based models—decision trees (DT), random forest (RF), and support vector machine (SVM)—and linear discriminant analysis (LDA) as a conventional model. Both cases of developing and non-developing tropical disturbances from the Joint Typhoon Warning Center (JTWC) best track were collected to train the models. The results of all accuracy metrics showed a higher performance for the ML models than for the LDA model. In particular, the ML models were able to detect TC initiation 26–30 h before a TC was diagnosed as a tropical depression, which was 5–9 h earlier than the detection by LDA.

Ye et al. [10] proposed an original monitoring system for detecting debris flow by building a wireless accelerometer network and evaluated it over a mountainous area in Japan. Defining the phenomena of debris flow is challenging because of its drastic ignition and difficult access. A two-stage data analysis process with anomaly detection and debris flow identification was implemented in the framework. Signals were detected using a state-of-the-art machine learning approach, convolutional neural networks. The network of connected sensors was able to provide a process of debris flow from the initial to final stages. The system developed suggested an alternative method to detect the disaster and the related analytical method.

Lee et al. [11] developed machine learning models to estimate the total precipitable water (TPW) from Himawari-8 data using the ERA-Interim TPW as a reference for Northeast Asia under the clear sky condition. The radiative transfer model was used for cloud screening. TPW, a column of water vapor content in the atmosphere, can be a critical variable to delineate hydrological conditions. It is also related to the intensity of disasters regarding the convective available potential energy (CAPE). Machine learning methods, RF, extreme gradient boosting (XGB), and deep neural network (DNN) were evaluated and compared. The DNN result outperformed the other models when validated using ERA-Interim and radiosonde observation (RAOB) data. TPWs retrieved from geostationary satellite images with a 10 min interval can provide valuable input to a disaster management system focusing on heavy rains and floods.

**Conflicts of Interest:** The authors declare no conflict of interest.

## References

1. Myoung, B.; Kim, S.; Nghiem, S.; Jia, S.; Whitney, K.; Kafatos, M. Estimating live fuel moisture from MODIS satellite data for wildfire danger assessment in Southern California USA. *Remote Sens.* **2018**, *10*, 87. [[CrossRef](#)]
2. Ryu, J.H.; Han, K.S.; Hong, S.; Park, N.W.; Lee, Y.W.; Cho, J. Satellite-based evaluation of the post-fire recovery process from the worst forest fire case in South Korea. *Remote Sens.* **2018**, *10*, 918. [[CrossRef](#)]
3. Yang, Q.; Ke, Y.; Zhang, D.; Chen, B.; Gong, H.; Lv, M.; Zhu, L.; Li, X. Multi-scale analysis of the relationship between land subsidence and buildings: a case study in an Eastern Beijing urban area using the PS-InSAR technique. *Remote Sens.* **2018**, *10*, 1006. [[CrossRef](#)]
4. Lim, J.; Lee, K.S. Flood mapping using multi-source remotely sensed data and logistic regression in the heterogeneous mountainous regions in North Korea. *Remote Sens.* **2018**, *10*, 1036. [[CrossRef](#)]
5. Ma, M.; Liu, C.; Zhao, G.; Xie, H.; Jia, P.; Wang, D.; Wang, H.; Hong, Y. Flash flood risk analysis based on machine learning techniques in the Yunnan province, China. *Remote Sens.* **2019**, *11*, 170. [[CrossRef](#)]
6. Jang, E.; Kang, Y.; Im, J.; Lee, D.W.; Yoon, J.; Kim, S.K. Detection and monitoring of forest fires using Himawari-8 geostationary satellite data in South Korea. *Remote Sens.* **2019**, *11*, 271. [[CrossRef](#)]
7. Zhang, J.; Zhang, Q.; Bao, A.; Wang, Y. A new remote sensing dryness index based on the near-infrared and red spectral space. *Remote Sens.* **2019**, *11*, 456. [[CrossRef](#)]
8. Zuo, J.; Gong, H.; Chen, B.; Liu, K.; Zhou, C.; Ke, Y. Time-series evolution patterns of land subsidence in the eastern Beijing Plain, China. *Remote Sens.* **2019**, *11*, 539. [[CrossRef](#)]

9. Kim, M.; Park, M.S.; Im, J.; Park, S.; Lee, M.I. Machine learning approaches for detecting tropical cyclone formation using satellite data. *Remote Sens.* **2019**, *11*, 1195. [[CrossRef](#)]
10. Ye, J.; Kurashima, Y.; Kobayashi, T.; Tsuda, H.; Takahara, T.; Sakurai, W. An efficient in-situ debris flow monitoring system over a wireless accelerometer network. *Remote Sens.* **2019**, *11*, 1512. [[CrossRef](#)]
11. Lee, Y.; Han, D.; Ahn, M.H.; Im, J.; Lee, S.J. Retrieval of total precipitable water from Himawari-8 AHI data: a comparison of random forest, extreme gradient boosting, and deep neural network. *Remote Sens.* **2019**, *11*, 1741. [[CrossRef](#)]



© 2019 by the authors. Licensee MDPI, Basel, Switzerland. This article is an open access article distributed under the terms and conditions of the Creative Commons Attribution (CC BY) license (<http://creativecommons.org/licenses/by/4.0/>).